Materials Science

http://www.aimspress.com/journal/Materials/

AIMS Materials Science, 4(2): 302-316.
DOI: 10.3934/matersci.2017.2.302
Received: 04 December 2016
Accepted: 04 February 2017
Published: 10 February 2017

Research article

Assessment of the interaction between three collinear unequal straight cracks with unified yield zones

N. Akhtar * **and S. Hasan**

Department of Mathematics, Jamia Millia Islamia, New Delhi-110 025, India

* **Correspondence:** Email: naved.a86@gmail.com.

Abstract: The Dugdale model has been modified in the paper to include the effect of linearly varying yield stress distribution. An isotropic infinite plate is considered with three collinear unequal straight cracks with coalesced yield zones. Muskhelishvili's complex variable approach is used to solve the problem. Closed form analytical expressions for stress intensity factor and crack tip opening displacement at each crack tip are obtained when boundary of the plate is subjected to uniform stress distribution and developed yield zones are assumed variable stress distribution. Different yield zone lengths and crack tip opening displacements are observed at each crack tip. A comparative case with the solution of two equal cracks is studied to show that the problem considered in this paper is the predecessor of the two equal cracks problem.

Keywords: multiple-site damage; stress intensity factor; yield zone length; Dugdale strip yield model; crack-tip opening displacement

Nomenclature

$\pm a_1, \pm b_1, c_1, d_1$	crack tips
$\pm a, \pm b$	tips of the developed yield plastic zones
$D_i\ (i = 0, 1, 2, 3)$	constants of the problem
E	Young's modulus
$F(\theta, k), E(\theta, k), \Pi(\theta, \alpha^2, k)$	incomplete elliptic integral of first, second, third kind, respectively
$L_i\ (i = 1, 2, 3)$	cracks
$P_n(z)$	polynomial of degree n
$p(t), q(t)$	applied stresses on the yield zones
u, v	components of displacement
X_x, Y_y, X_y	components of stress

Nomenclature

$z = x + iy$	complex variable
γ	Poisson's ratio
μ	shear modulus
$\delta(x)$	crack-tip-opening displacement at the crack tip x
$\Omega(z) = \omega'(z), \Phi(z) = \phi'(z)$	complex stress functions
Γ'	$-\frac{1}{2}(N_1 - N_2)e^{-2i\alpha}, N_1$ and N_2 are the values of principal stresses at infinity, α be the angle between N_1 and the ox-axis
$\Gamma_i\ (i = 1, 2, \ldots, 6)$	developed plastic/yield zones
κ	$= \frac{3-\gamma}{1+\gamma}$ for the plane-stress, $= 3 - 4\gamma$ for the plane-strain
σ_∞	remotely applied stress at infinite boundary of the plate
σ_{ye}	yield stress of the plate

1. Introduction

Sometimes man-made structures are catastrophic due to decreasing the residual strength of the material used for the development and propagation of cracks or crack like defects [1]. Human life sometimes is in danger since these structures break unconditionally. A number of aircraft and ships were failed at initial stage due to the presence of multiple interacting cracks in the manufactured structures. Therefore, it becomes imperative to study the load bearing capacity of the plate containing defects. Dugdale [2] proposed a classical single crack model to evaluate load carrying capacity of a plate. This model was used and modified by Kanninen [3] for linear stress distribution. Effect of variable stress distribution on the rims of developed yield zones studied by Harrop [4].

Cracks in the structure increase initially as non-interacting and isolated defects. As the length of cracks increases (in other words distance between cracks decreases) a destructive interaction between cracks increases rapidly causes the failure of the structures. So the available results of single crack are not appropriate for the modelling of multiple site damage problem [5]. Hence, Collins et al. [6] and Chang et al. [7] applied Dugdale model to obtain the solution of two equal straight cracks in an infinite plate, they also discussed the conditions of coalescence of yield zones between cracks. Dugdale strip yield model for three collinear straight cracks was studied by Hasan et al. [8] and further modified the model for linear stress distribution [9].

Many efforts, in fact, have been made for the case of separated yield zones as far as multiple cracks are the concern. However, some efforts have been made by various researchers [10, 11] to investigate the load bearing capacity of the cracked plate when yield zones were coalesced due to increase in applied stresses. As discussed by Gdoutos [12] that some of the structure fail at a stress, which is below the yield stress of the plate. Therefore, assuming the variable stress distribution acting on the rims of yield zones in order to arrest the cracks from further opening. Few cases of linear stress distribution have been considered by Tang et al. [13], Hasan [14] and Tada et al. [15]. Therefore, the purpose of this work is to study the interaction of multiple cracks when yield zones developed between two closely located cracks coalesced under the application of linearly varying stress distribution.

2. Basic Mathematical Formulation

Components of stresses (X_x, Y_y, X_y) and displacements (u, v) are same as given by Muskhelishvili [16] in terms of two complex potential functions $\Phi(z), \Omega(z)$ as

$$X_x + Y_y = 2[\Phi(z) + \overline{\Phi(z)}], \tag{1}$$
$$Y_y - iX_y = \Phi(z) + \overline{\Omega(z)} - (z - \bar{z})\Phi'(z), \tag{2}$$
$$2\mu(u + iv) = \chi\phi(z) - z\overline{\phi'(z)} - \overline{\psi(z)}. \tag{3}$$

where bar over the function or variable denotes its complex conjugate and *prime* its first order derivative.

If the stresses $X_y^{\pm}, Y_y^{\pm}$ are applied over the rims of the cracks, where superscript (+) & (−) denotes the values of stress components on the upper and lower rims of the cracks, the boundary value problem may be expressed as

$$Y_y^+ - iX_y^+ = \Phi^+(t) + \Omega^-(t), \tag{4}$$
$$Y_y^- - iX_y^- = \Phi^-(t) + \Omega^+(t), \tag{5}$$

under the assumption $\lim_{y\to 0} y\Phi'(t + iy) = 0$.

General solution of the boundary value problems given in Eqs. (4) and (5) is obtained using Sokhotski Plemelj formula and written as

$$\Phi(z) + \Omega(z) = \frac{1}{\pi i X(z)} \int_L \frac{X(t)p(t)dt}{t - z} + \frac{2P_n(z)}{X(z)}, \tag{6}$$
$$\Phi(z) - \Omega(z) = \frac{1}{\pi i} \int_L \frac{q(t)dt}{t - z} - \overline{\Gamma'}, \tag{7}$$

where

$$p(t) = \frac{1}{2}[Y_y^+ + Y_y^-] - \frac{i}{2}[X_y^+ + X_y^-], \quad q(t) = \frac{1}{2}[Y_y^+ - Y_y^-] - \frac{i}{2}[X_y^+ - X_y^-],$$
$$X(z) = \prod_{j=1}^{n} \sqrt{z - a_j}\sqrt{z - b_j}, \quad P_n(z) = D_0 z^n + D_1 z^{n-1} + D_2 z^{n-2} + \cdots + D_n,$$

a_j, b_j are the end points of j^{th} crack.

Unknown constants D_i $(i = 0, 1, 2, \ldots, n)$ of polynomial $P_n(z)$ may be obtained using condition of single-valuedness of displacement around the rims of the cracks,

$$2(\chi + 1) \int_{L_i} \frac{P_n(t)}{X(t)} dt + \chi \int_{L_i} [\Phi_0^+(t) - \Phi_0^-(t)]dt + \int_{L_i} [\Omega_0^+(t) - \Omega_0^-(t)]dt = 0. \tag{8}$$

3. Problem Formulation

The present analysis is a modification of Dugdale model under the influence of linear stress distribution. Consider a plate is to be infinitely extended and contains three unequal cracks L_1, L_2, L_3 of real lengths $(-a_1, -b_1)$, (b_1, c_1), (d_1, a_1) along the x-axis. Boundary of the plate is subjected to uniform stress distribution, $Y_y = \sigma_\infty$ opens the rims of the cracks in mode-I type deformation. As a result, at each crack tip yield zone develop and grow on increasing stresses at the boundary of the plate. Therefore, yield zones developed at interior tips of two closely located cracks get coalesced. These zone are denoted by Γ_i $(i = 1, 2, 3, \ldots, 6)$ and occupy the intervals $(-a, -a_1)$, $(-b_1, -b)$, (b, b_1), (c_1, d_1), (a_1, a) respectively, on *ox-axis*.

Further damage in the plate is seized by applying a linear stress distribution $Y_y = \frac{t}{a}\sigma_{ye}$ over the rims of developed yield zones. The entire configuration of this problem is given in Figure 1.

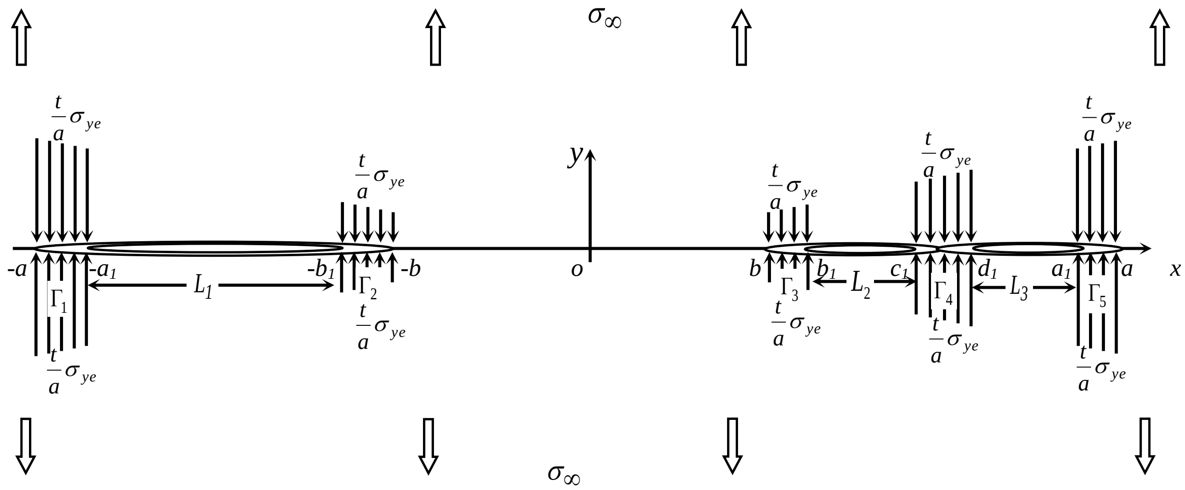

Figure 1. Configuration of the problem.

4. Solution to the Problem

The solution of the problem stated in Section 3 is obtained by superposition solution of two states of the problem. The first state is the tensile case when the infinite boundary is subjected to uniform stress distribution. The second state of the problem is to apply a linear stress distribution on the rims of the yield zones.

4.1. State-1: Tensile Case

Consider, two cracks exist on the real axis in an infinite plate which is subjected to uniform tension, σ_∞. The entire configuration is shown in Figure 2.

The problem of tensile case is solved under the following boundary conditions,

$$Y_y = \sigma_\infty, X_y = 0, \qquad for \quad y \to \pm\infty, -\infty < x < \infty \tag{9}$$

$$Y_y = X_y = 0, \qquad for \quad y = 0, x \in \bigcup_{i=1}^{2} R_i \tag{10}$$

The desired complex potential function $\Phi_A(z)$ for this case is calculated using mathematical formulation given in Section 2 and boundary conditions (9) and (10) as,

$$\Phi_A(z) = \frac{\sigma_\infty}{2}\Big[\frac{1}{X(z)}(z^2 - a^2\lambda^2) - \frac{1}{2}\Big] \tag{11}$$

where $\lambda^2 = \frac{E(k)}{F(k)}, k^2 = \frac{a^2-b^2}{a^2}$ and $F(k), E(k)$ are complete elliptical integrals of first and second kind, respectively, defined in Byrd [17].

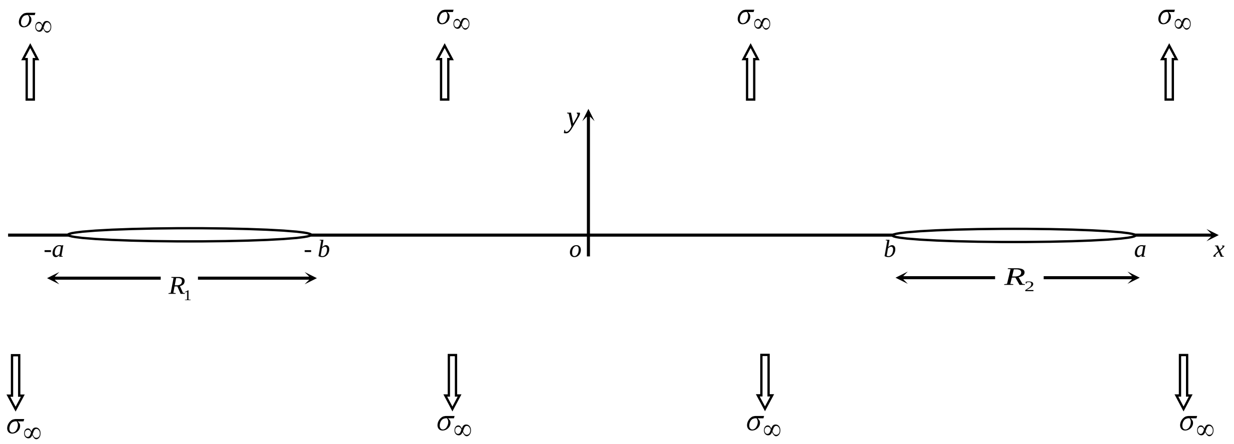

Figure 2. Configuration of the tensile case.

Formula given here of calculating stress intensity factors for the configuration of Figure 2 at crack tip $z = z_1$ is taken from [6],

$$K_I \quad = \quad 2\sqrt{2\pi}\lim_{z\to z_1}\sqrt{z - z_1}\,\Phi_A(z). \tag{12}$$

Hence, opening mode stress intensity factors at crack tips a and b are determine by substituting $\Phi_A(z)$ from Eq. (11) into Eq. (12) and after taking corresponding limits one can write

$$(K_I^A)_a \quad = \quad \sigma_\infty\sqrt{\frac{\pi}{a}}\frac{a^2}{\sqrt{a^2 - b^2}}(1 - \lambda^2), \tag{13}$$

$$(K_I^A)_b \quad = \quad \sigma_\infty\sqrt{\frac{\pi}{b}}\frac{1}{\sqrt{a^2 - b^2}}(b^2 - a^2\lambda^2), \tag{14}$$

where subscript I refers to mode-I type deformation, and superscript A refers to *sub-problem-A*.

Displacement components for the tensile case is obtained on putting the value of $\Phi_A(z)$ from Eq. (11) into Eq. (3) as,

$$(v_A^\pm)_a \quad = \quad \pm\frac{2a\sigma_\infty}{E}\Big[E(\theta_1, k) - \lambda^2 F(\theta_1, k)\Big], \tag{15}$$

$$(v_A^\pm)_b \quad = \quad \mp\frac{2a\sigma_\infty}{E}\Big[E(\theta_2, k) - \lambda^2 F(\theta_2, k) - \frac{k^2\sin\theta_2\cos\theta_2}{\sqrt{1 - k^2\sin^2\theta_2}}\Big], \tag{16}$$

where $\theta_1 = sin^{-1}\sqrt{\frac{a^2-a_1^2}{a^2-b^2}}, \quad \theta_2 = sin^{-1}\sqrt{\frac{a^2-b_1^2}{a^2-b^2}}$.

4.2. State-2: Yield Case

In this section, we aim to furnish a mathematical model for an isotropic infinite plate which is damaged by three collinear straight cracks with coalesced yield zones at the interior tip of two closely located cracks tips. These cracks are assumed to be located along *ox*-axis and denoted by L_i $(i = 1, 2, 3)$. Cracks together with corresponding yield zones are treated as physical cracks of length $(\Gamma_1 \bigcup L_1 \bigcup \Gamma_2)$, and $(\Gamma_3 \bigcup L_2 \bigcup \Gamma_4 \bigcup L_3 \bigcup \Gamma_5)$. The model may be illustrated by means of Figure 3. Rims of developed yield zones are subjected to a compressive stress distribution to detain the cracks from further opening. According to Godoutos [12], in history, a number of failures occurred at a stress which is well below the yield strength of the plate. Therefore a linearly varying stress $\frac{t}{a}\sigma_{ye}$ (stress which is below the yield strength of the plate) distribution is considered over the rims of developed yield zones.

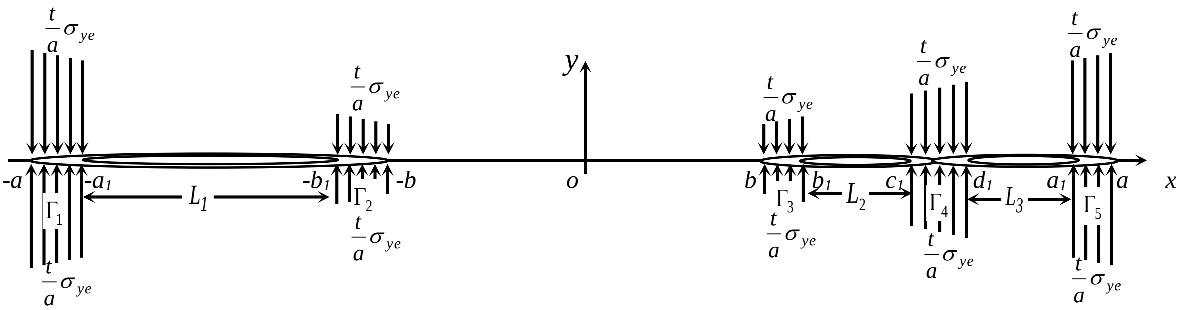

Figure 3. Configuration of the yield case.

The boundary conditions of the said problem are:

$$Y_y = 0, X_y = 0, \qquad for \quad y \to \pm\infty, -\infty < x < \infty \tag{17}$$

$$Y_y = \frac{t}{a}\sigma_{ye}, \quad X_y = 0, \qquad for \quad y \to 0, x \in \bigcup_{n=1}^{6} \Gamma_n \tag{18}$$

Using methodology given in Section 2 and boundary conditions (17) and (18), complex potential function for the *sub-problem-B* is obtained and written as:

$$\Phi_B(z) \quad = \quad \frac{\sigma_{ye}}{2\pi i X(z)}\Big[\int_{L'} \frac{tX(t)dt}{a(t-z)} + iD_2\Big] \tag{19}$$

where $L' = [-a, -a_1] \bigcup [-b_1, -b] \bigcup [b, b_1] \bigcup [c_1, d_1] \bigcup [a_1, a]$, i.e., the loaded section in Figure 3.

Using the fact that,

$$X(t) \quad = \quad \sqrt{t-a}\,\sqrt{t+a}\,\sqrt{t-b}\,\sqrt{t+b} = i\,\sqrt{a^2-t^2}\,\sqrt{t^2-b^2}, \tag{20}$$

$$X(-t) \quad = \quad \sqrt{-t-a}\,\sqrt{-t+a}\,\sqrt{-t-b}\,\sqrt{-t+b} = -i\,\sqrt{a^2-t^2}\,\sqrt{t^2-b^2}. \tag{21}$$

The integral shown in Eq. (19) may be evaluated as,

$$\int_{L'} \frac{tX(t)dt}{a(t-z)} \quad = \quad \frac{2}{a}\int_{a_1}^{a} \frac{t^2X(t)}{t^2-z^2}dt + \frac{2}{a}\int_{b}^{b_1} \frac{t^2X(t)}{t^2-z^2}dt + \frac{1}{a}\int_{c_1}^{d_1} \frac{(t^2+tz)X(t)}{t^2-z^2}dt,$$

$$= \frac{2i}{a}\Big[\int_{a_1}^{a} \frac{t^2\sqrt{a^2-t^2}\sqrt{t^2-b^2}}{t^2-z^2}dt + \int_{b}^{b_1} \frac{t^2\sqrt{a^2-t^2}\sqrt{t^2-b^2}}{t^2-z^2}dt$$
$$+\frac{1}{2}\int_{c_1}^{d_1} \frac{t^2\sqrt{a^2-t^2}\sqrt{t^2-b^2}}{t^2-z^2}dt + \frac{z}{2}\int_{c_1}^{d_1} \frac{t\sqrt{a^2-t^2}\sqrt{t^2-b^2}}{t^2-z^2}dt\Big],$$

Hence,

$$\int_{L'} \frac{tX(t)dt}{a(t-z)} = 2ia^2k^2\Big[I_1 + \Big(1-\frac{1}{n^2}\Big)J_1 + \frac{z}{a}\Big\{I_2 + \Big(1-\frac{1}{n^2}\Big)J_2\Big\}\Big], \tag{22}$$

where

$$\begin{aligned}
I_1 &= i_1(\theta_1) - i_1(\theta_2) + i_1\Big(\frac{\pi}{2}\Big) + \frac{1}{2}\Big(i_1(\theta_3) - i_1(\theta_4)\Big),\\
J_1 &= j_1(\theta_1) - j_1(\theta_2) + j_1\Big(\frac{\pi}{2}\Big) + \frac{1}{2}\Big(j_1(\theta_3) - j_1(\theta_4)\Big),\\
I_2 &= \frac{1}{2}\Big(i_2(\theta_3) - i_2(\theta_4)\Big), \quad J_2 = \frac{1}{2}\Big(j_2(\theta_3) - j_2(\theta_4)\Big),\\
n^2 &= \frac{a^2-b^2}{a^2-z^2}, \quad \theta_3 = sin^{-1}\sqrt{\frac{a^2-c_1^2}{a^2-b^2}}, \quad \theta_4 = sin^{-1}\sqrt{\frac{a^2-d_1^2}{a^2-b^2}},\\
i_1(\phi) &= \frac{1}{3k^2}\Big[(1-k^2)F(\phi,k) + (2k^2-1)E(\phi,k) - k^2\sin\phi\cos\phi\sqrt{1-k^2\sin^2\phi}\Big],\\
j_1(\phi) &= \Big[\frac{k^2}{n^2}F(\phi,k) - E(\phi,k) + \frac{n^2-k^2}{n^2}\Pi(\phi,n,k)\Big],\\
i_2(\phi) &= \frac{1}{2}(\phi - \sin\phi\cos\phi), \quad j_2(\phi) = \Big[\frac{\tanh^{-1}\Big(\sqrt{n^2-1}\tan\phi\Big)}{\sqrt{n^2-1}} - \phi\Big].
\end{aligned}$$

Constant D_2 is then obtained by using condition of single-valuedness of displacement around the rims of cracks given and written as ,

$$D_2 = -2a^2k^2(T_1 - \lambda^2 T_2), \tag{23}$$

where

$$\begin{aligned}
T_1 &= t_1(\theta_1) - t_1(\theta_2) + t_1(\frac{\pi}{2}) + \frac{1}{2}t_1(\theta_3) - \frac{1}{2}t_1(\theta_4),\\
T_2 &= t_2(\theta_1) - t_2(\theta_2) + t_2(\frac{\pi}{2}) + \frac{1}{2}t_2(\theta_3) - \frac{1}{2}t_2(\theta_4),\\
t_1(\phi) &= \frac{\sin\phi\cos\phi\sqrt{1-k^2\sin^2\phi}}{6} - \frac{1-k^2}{6k^2}F(\phi,k) + \Big(\frac{2-k^2}{3k^2} - \frac{1-k^2\sin^2\phi}{2k^2}\Big)E(\phi,k)\\
t_2(\phi) &= \frac{E(\phi,k)}{2k^2} - \frac{1-k^2\sin^2\phi}{2k^2}F(\phi,k).
\end{aligned}$$

Thus, after a long mathematical calculations, final expressions for complex potential function $\Phi_B(z)$ of closing case is obtained on substituting Eqs. (22) and (23) into Eq. (19),

$$\Phi_B(z) \;=\; \frac{a^2k^2\sigma_{ye}}{\pi X(z)}\Big[I_1 + (1-\frac{1}{n^2})J_1 + \frac{z}{a}\Big(I_2 + (1-\frac{1}{n^2})J_2\Big) - (T_1 - \lambda^2 T_2)\Big], \tag{24}$$

Stress intensity factors at crack tips *a, b* for linear stress distribution is obtained by putting the value of $\Phi_B(z)$ from Eq. (24) into Eq. (12), therefore

$$(K_I^B)_a \;=\; \frac{2a^2k^2\sigma_{ye}}{\sqrt{a\pi}\,\sqrt{a^2-b^2}}\Big(I_1 - E_1 + I_2 - \phi_1 - (T_1 - \lambda^2 T_2)\Big), \tag{25}$$

$$(K_I^B)_b \;=\; \frac{2a^2k^2\sigma_{ye}}{\sqrt{b\pi}\,\sqrt{a^2-b^2}}\Big(I_1 + \frac{b}{a}I_2 - (T_1 - \lambda^2 T_2)\Big). \tag{26}$$

where

$$E_1 \;=\; E(\theta_1,k) - E(\theta_2,k) + E(\frac{\pi}{2},k) + \frac{1}{2}E(\theta_3,k) - \frac{1}{2}E(\theta_4,k), \quad \phi_1 = \frac{1}{2}\theta_3 - \frac{1}{2}\theta_4$$

Components of displacement are obtained on putting the value of $\Phi_B(z)$ in Eq. (3),

$$(v_B^{\pm})_{a_1} \;=\; \pm\frac{4a}{\pi E}\Big(A_1 + A_2\Big), \tag{27}$$

$$(v_B^{\pm})_{b_1} \;=\; \mp\frac{4a}{\pi E}\Big(B_1 + B_2\Big), \tag{28}$$

where

$$\begin{aligned}
A_1 \;=\;& \Big\{I_1 - (T_1 - \lambda^2 T_2)\Big\}F(\theta_1,k)k^2 - \frac{F_1}{2}\Big\{(1-k^2)F(\theta_1,k) + k^2 S(\theta_1)\Big\} + \\
& I_2 k^2\theta_1 - \frac{\phi_1 k^2}{2}\Big\{\frac{\sin 2\theta_1}{2} + \theta_1\Big\} - \frac{E_1}{2}\Big\{E(\theta_1,k) - 2(1-k^2)F(\theta_1,k)\Big\}, \\
A_2 \;=\;& \frac{a_1^3\sqrt{a_1^2-b^2}}{2a^3\sqrt{a^2-a_1^2}}\Big\{\Pi(\theta_2,\alpha^2(a_1),k) - \Pi(\frac{\pi}{2},\alpha^2(a_1),k) - \frac{1}{2}\Pi(\theta_3,\alpha^2(a_1),k) + \frac{1}{2}\Pi(\theta_4,\alpha^2(a_1),k)\Big\} \\
& + \frac{1}{2}\Big\{\frac{1}{2}S(\theta_3)\Lambda_1(c_1) - S(\theta_2)\Lambda_1(b_1) - \frac{1}{2}S(\theta_4)\Lambda_1(d_1)\Big\} + \frac{1}{2a^2}\Big\{\Lambda_2(c_1) - \Lambda_2(d_1)\Big\}, \\
B_1 \;=\;& \Big\{I_1 - (T_1 - \lambda^2 T_2)\Big\}F(\theta_5,k)k^2 + \frac{F_1}{2}\Big\{N(\theta_5) - (1-k^2)F(\theta_5,k)\Big\} - \\
& \frac{k^2\phi_1}{2}\Big\{\frac{\pi}{2} - \frac{\sin 2\theta_2}{2} - \theta_2\Big\} - \frac{E_1}{2}\Big\{M(\theta_5) - 2(1-k^2)F(\theta_5,k)\Big\} + k^2 I_2\Big\{\frac{\pi}{2} - \theta_2\Big\}, \\
B_2 \;=\;& \frac{b_1^3\sqrt{b_1^2-b^2}}{2a^3\sqrt{a^2-b_1^2}}\Big\{\Pi(\theta_1,\alpha^2(b_1),k) + \Pi(\frac{\pi}{2},\alpha^2(b_1),k) + \frac{1}{2}\Pi(\theta_3,\alpha^2(b_1),k) - \frac{1}{2}\Pi(\theta_4,\alpha^2(b_1),k)\Big\} \\
& + \frac{b^2k^2}{2}\Big\{S(\theta_1)\Lambda_3(a_1) + \frac{1}{2}S(\theta_3)\Lambda_3(c_1) - \frac{1}{2}S(\theta_4)\Lambda_3(d_1)\Big\} + \frac{1}{2a^2}\Big\{\Lambda_4(c_1) - \Lambda_4(d_1)\Big\},
\end{aligned}$$

$$
\begin{aligned}
F_1 &= F(\theta_1,k) - F(\theta_2,k) + F(\frac{\pi}{2},k) + \frac{1}{2}F(\theta_3,k) - \frac{1}{2}F(\theta_4,k), \quad \alpha_1^2(t) = \frac{t^2(a^2-b^2)}{a^2(t^2-b^2)},\\
\theta_5 &= \sin^{-1}\sqrt{\frac{a^2(b_1^2-b^2)}{b_1^2(a^2-b^2)}}, \quad S(\theta) = \sin\theta\cos\theta\sqrt{1-k^2\sin^2\theta}, \quad \alpha^2(t) = \frac{a^2-b^2}{a^2-t^2},\\
M(\theta) &= E(\theta,k) - \frac{k^2\sin\theta\cos\theta}{\sqrt{1-k^2\sin^2\theta}}, \quad N(\theta) = \frac{k^2(1-k^2)}{(1-k^2\sin^2\theta)^{\frac{3}{2}}},\\
\Lambda_1(t) &= (\alpha^2(t)-k^2)\pi(\theta_1,\alpha^2(t),k) + k^2F(\theta_1,k), \quad \Lambda_2(t) = -\xi(t,a_1) - \frac{iX(t)}{2k^2}\Big(k^2\theta_1 + \zeta(t,\theta_1)\Big),\\
\Lambda_3(t) &= \frac{1}{t^2-b^2}\Pi(\theta_5,\alpha_1^2(t),k), \quad \Lambda_4(t) = \xi(t,b_1) - \frac{iX(t)}{2k^2}\Big(k^2\Big(\frac{\Pi}{2}-\theta_2\Big) - \zeta(t,\theta_2)\Big),\\
\xi(\beta,\gamma) &= \frac{\gamma^2}{2}\tanh^{-1}\sqrt{\frac{(a^2-\beta^2)(\gamma^2-b^2)}{(a^2-\gamma^2)(\beta^2-b^2)}}, \quad \zeta(\beta,\gamma) = \frac{(\alpha^2(\beta)-k^2)\tanh^{-1}(\sqrt{\alpha^2(\beta)-1}\tan\gamma)}{\sqrt{\alpha^2(\beta)-1}}.
\end{aligned}
$$

5. Illustrative Study: Yield Zone Length and Crack-tip Opening Displacement

The techniques outlined have been used to evaluate yield zone lengths and crack tip opening displacements for three cracks with coalesced yield zones under linearly varying stress distribution. Yield zone length at each crack tip is evaluated using Dugdale [2] hypothesis that the stresses remain finite in the vicinity of crack, hence

$$K = K_I^A(z_1) + K_I^B(z_1) = 0. \tag{29}$$

On substituting the corresponding values of K_I^A from Eqs. (13) and (14) and the values of K_I^B from Eqs. (25) and (26) into Eq. (29), one may get two non-linear equations as given below.

$$\Big(\frac{\sigma_\infty}{\sigma_{ye}}\Big)_a(1-\lambda^2) + \frac{2k^2}{\pi}\Big[I_1 - E_1 + I_2 - \phi_1 - (T_1 - \lambda^2T_2)\Big] = 0, \tag{30}$$

$$\Big(\frac{\sigma_\infty}{\sigma_{ye}}\Big)_b(b^2 - a^2\lambda^2) + \frac{2a^2k^2}{\pi}\Big[I_1 + \frac{b}{a}I_2 - (T_1 - \lambda^2T_2)\Big] = 0. \tag{31}$$

It is almost impossible to obtain yield zone length for prescribed values of $\frac{\sigma_\infty}{\sigma_{ye}}$, therefore $\frac{\sigma_\infty}{\sigma_{ye}}$ is evaluated for given value of $|b_1 - b|, |d_1 - c_1|$ and $|a - a_1|$. Figure 4 shows the variation between normalized load ratio $\frac{\sigma_\infty}{\sigma_{ye}}$ and normalized yield zone length $\frac{|a-a_1|}{|a_1-b_1|}$ for different values of $\frac{a_1-b_1}{a_1+b_1}$ (say $\triangle$). It is clearly observed as the load applied at the boundary of the plate increases yield zone length $|a - a_1|$ increases as expected. The results of three collinear straight cracks with coalesced yield zones are compared with the results of two equal collinear cracks of the same length under same loading conditions, a significant difference is seen in yield zone length when cracks L_1 and L_2 are located far away from each other.

Figure 5 shows the increase in the length of yield zone at crack tip b when applied stresses increases. It is seen from the graph, yield zone length $|b_1 - b|$ is highly affected by the presence of another crack. The plate can bear more load when cracks are located far away ($\triangle = 0.1$) in comparison to closely located cracks ($\triangle = 0.9$). Furthermore, on comparing the results with two equal cracks it is clear that no significant difference is seen in bearing capacity for closely located cracks $k = 0.9$.

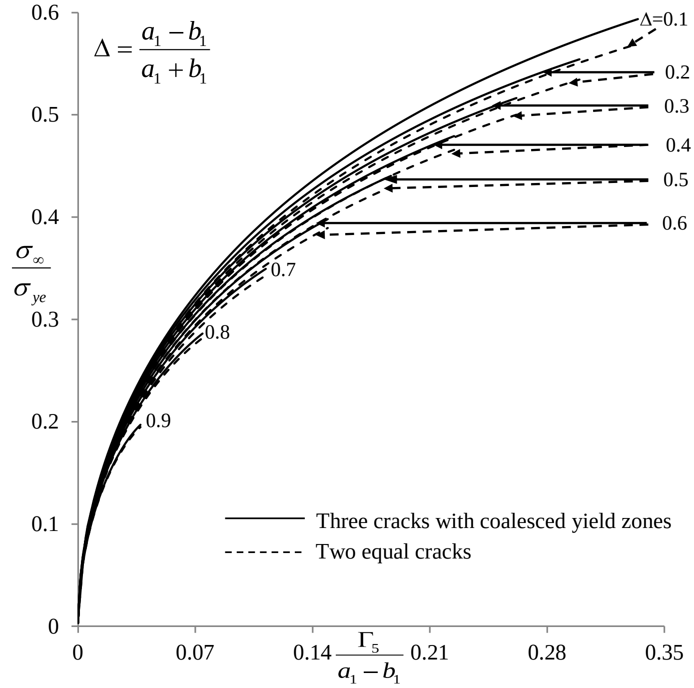

Figure 4. Variation between yield zone length and applied load ratio at the outer crack tip.

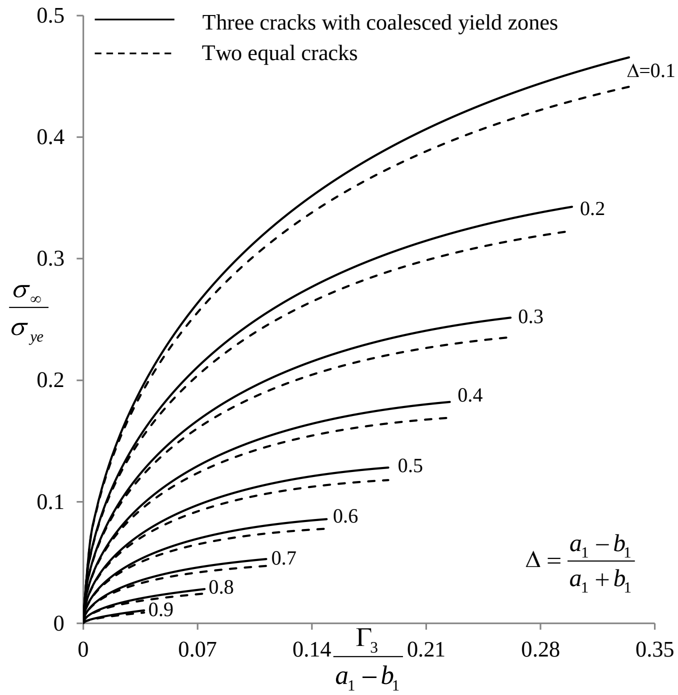

Figure 5. Variation between yield zone length and applied load ration at the inner crack tip.

Crack tip opening displacement (CTOD) is obtained using the formula given by Feng et al. [18],

$$\delta^{\pm}(x) \quad = \quad v_A^{\pm}(x) - v_B^{\pm}(x), \tag{32}$$

Hence, on substituting corresponding values of $v_A^{\pm}$ and $v_B^{\pm}$ from Eqs. (15) and (16) and Eqs. (27) and (28) into Eq. (32). One may get two non-linear equations for CTOD at crack tip a_1 and b_1, as

$$\delta^{\pm}(a_1) = \pm\frac{4a\sigma_{ye}}{E}\Big\{\Big(E(\theta_1,k)-\lambda^2F(\theta_1,k)\Big)\Big(\frac{\sigma_\infty}{\sigma_{ye}}\Big)_a-\frac{2}{\pi}\Big(A_1+A_2\Big)\Big\}, \tag{33}$$

$$\delta^{\pm}(b_1) = \mp\frac{4a\sigma_{ye}}{E}\Big\{\Big(E(\theta_2,k)-\lambda^2F(\theta_2,k)-\frac{k^2\sin\theta_2\cos\theta_2}{\sqrt{1-k^2\sin^2\theta_2}}\Big)\Big(\frac{\sigma_\infty}{\sigma_{ye}}\Big)_b-\frac{2}{\pi}\Big(B_1+B_2\Big)\Big\}. \tag{34}$$

In order to investigated CTODs shown in Eqs. (33) and (34) at crack tips a_1 and b_1 ratio of CTODs to crack length has been plotted against applied load ratio. Figure 6 shows the said variation at crack tip a_1 while Figure 7 at crack tip b_1.

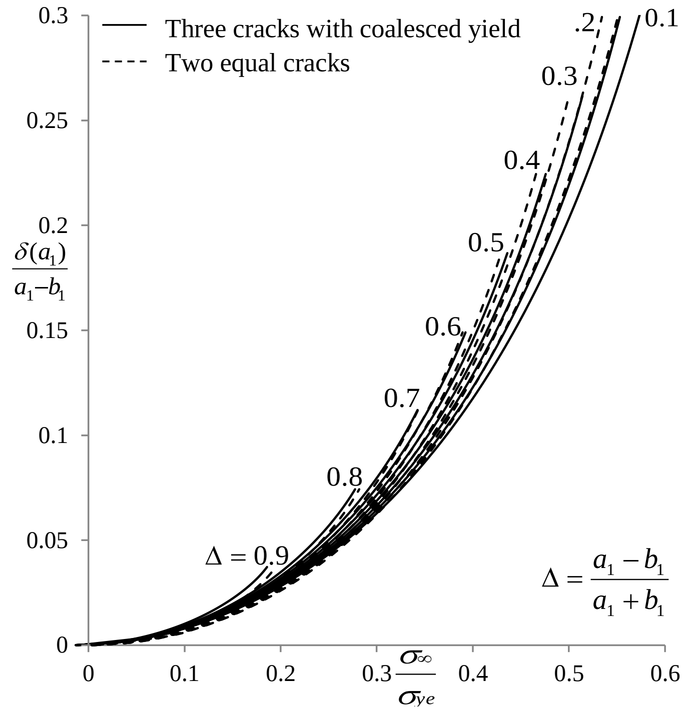

Figure 6. CTOD against applied load ratio at the crack tip a_1.

As the load applied at the boundary of the plate increases cracks open in mode-I type deformation. In the case of $\triangle = 0.9$ the opening of cracks are almost same in comparison to the opening of two equal cracks. But the opening at crack tip a_1 when $\triangle = 0.1$ is significantly different in the said comparison.

Figure 7 shows the behaviour of normalized CTOD with respect to applied load ratio $\frac{\sigma_\infty}{\sigma_{ye}}$ at inner crack tip b_1. CTOD at inner crack tip b_1 is increasing gradually as the applied load at the boundary of the plate is increased. Moreover, a significant difference is seen in the CTOD of two configurations for different values of $\triangle$.

A comparison of the results obtained is shown in Figure 8 and 9 with the results of single cracks given by Harrop [4]. It has been observed that as $\triangle = 0.9$, means cracks are located close to each other, behaviour of yield zone length and CTOD in case of configuration shown in Figure 1 is similar to single crack.

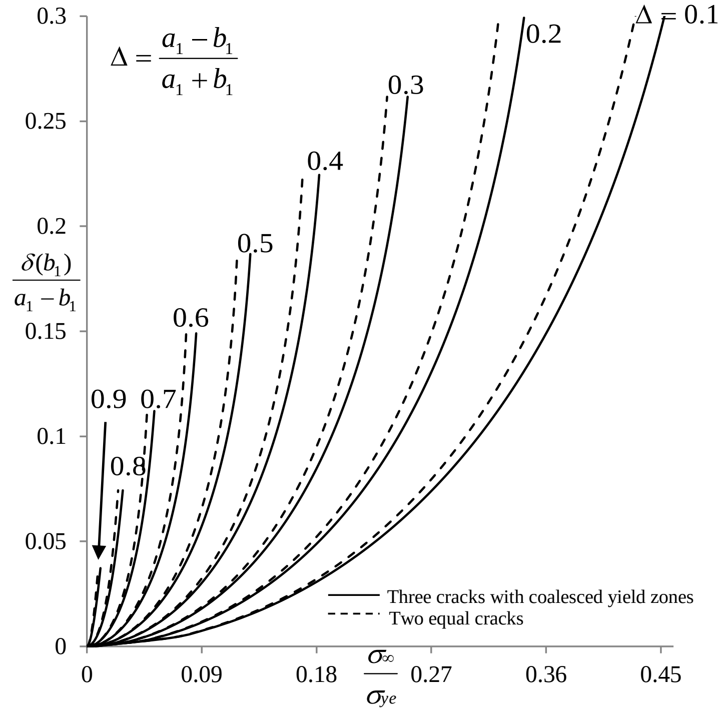

Figure 7. CTOD against applied load ratio at the crack tip b_1.

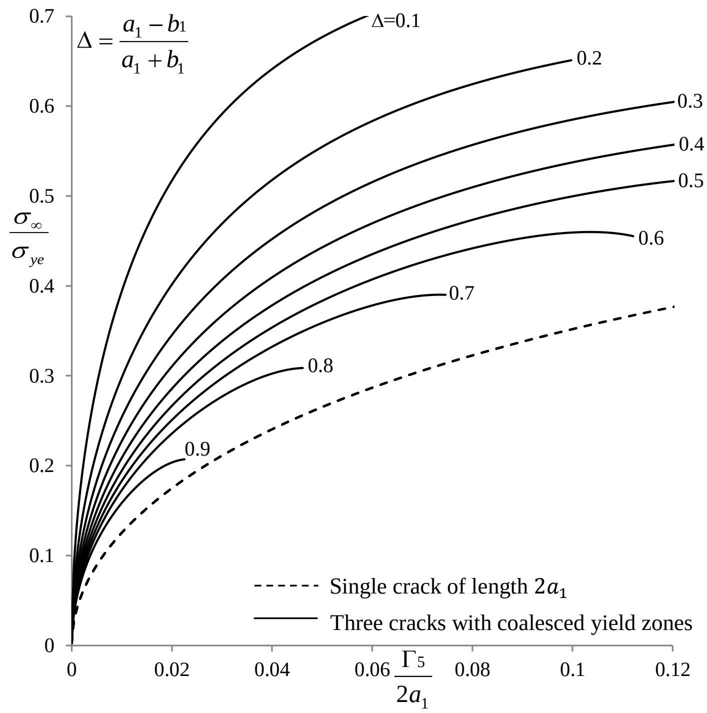

Figure 8. Comparison of yield Zone length with single crack

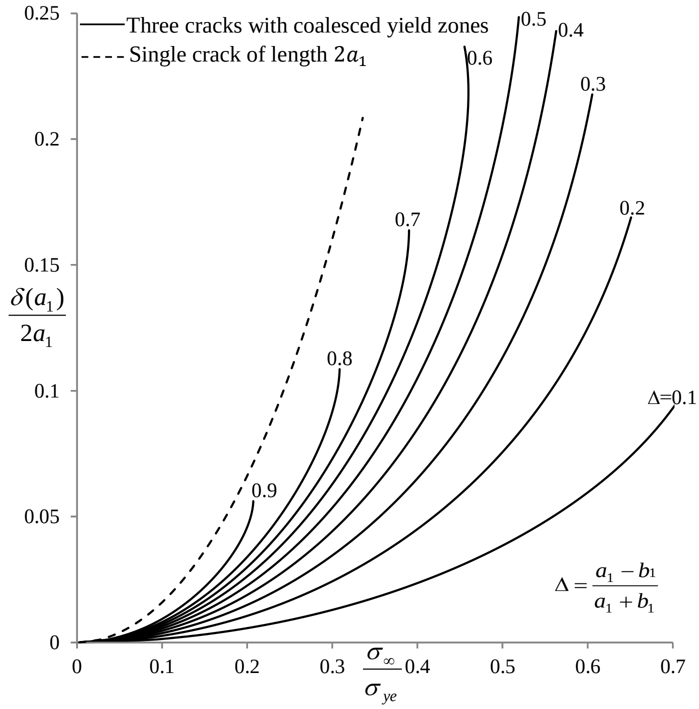

Figure 9. Comparison of CTOD with single crack

6. Validation of Results

1) Results of opening mode stress intensity factor for *sub problem A* given in Eqs. (13) and (14) are the same as given by Tada [15];

2) Expression of yield zone length given in Eq. (30) and crack-tip opening displacement in Eq. (33) are same as the expressions given by Harrop [4] taking $b = b_1 = c_1 = d_1 = 0$ for a single crack.

7. Conclusions

The following set of conclusions may be drawn from the work that has been reported. The problem of three asymmetrical collinear straight cracks with coalesced yield zones in an infinite sheet is analyzed.

a) Analytical expression for stress intensity factors, yield zone length and CTODs have been obtained under linearly varying stress distribution using the complex variable method.

b) Numerical results for applied stresses, the length of yield zones and crack-tip opening displacements are plotted and reported graphically. These results are compared with the results of an equivalent configuration of two equal collinear straight cracks.

c) It has been observed that the plate can bear more load when the coalesced yield zone Γ_5 bigger in size as compared to yield zone Γ_3.

d) Less opening of cracks is seen in the presence of coalesced yield zones when results are compared with the results of two equal cracks.

Acknowledgement

First author is also grateful to University Grant Commission(UGC) for providing financial support under UGC-BSR scheme.

Conflict of Interest

All authors declare no conflict of interest in this paper.

References

1. Broek D (1982) *Elementary Engineering Fracture Mechanics*, The Netherlands: Martinus Nijhoff.
2. Dugdale DS (1960) Yielding of steel sheets containing slits. *J Mech Phys Solids* 8: 100–104.
3. Kanninen MF (1970) A solution for a Dugdale crack subjected to a linearly varying tensile loading. *Int J Eng Sci* 8: 85–95.
4. Harrop LP (1978) Application of a modified Dugdale model to the K vs COD relation. *Eng Fract Mech* 10: 807–816.
5. Chang D, Kotousov A (2012) A strip yield model for two collinear cracks in plates of arbitrary thickness. *Int J Fracture* 176: 39 – 47.
6. Collins RA, Cartwright DJ (2001) An analytical solution for two equal-length collinear strips yield cracks. *Eng Fract Mech* 68: 915–924.
7. Chang Dh, Kotousov A (2012) A strip yield model for two collinear cracks. *Eng Fract Mech* 90: 121 – 128.
8. Hasan S, Akhtar N (2015) Dugdale model for three equal collinear straight cracks: An analytical approach. *Theor Appl Fract Mec* 78: 40 – 50.
9. Hasan S, Akhtar N (2015) Mathematical model for three equal collinear straight cracks: A modified Dugdale approach. *Strength Fract Complex* 9: 211 – 232.
10. Nishimura T (1999) Strip Yield Analysis on Coalescence of Plastic Zones for Multiple Cracks in a Riveted Stiffened Sheet. *ASME J Eng Mater Technol* 121: 352 – 359.
11. Hasan S (2015) Dugdale model for three unequal collinear straight cracks with coalesced yield zones: a complex variable approach. *Int J Pure Ap Mat* 105: 311 – 323.
12. Gdoutos EE (2005) *Fracture Mechanics–An Introduction*, Springer.
13. Tang XS, Gao CH (2014) Macromicro dual scale crack model linked by a restraining stress zone with a linear distribution. *Theor Appl Fract Mec* 71: 31 – 43.
14. Hasan S (2016) Modified Dugdale model for four collinear straight cracks with coalesced yield zones. *Theor Appl Fract Mec* 85: 227 – 235.
15. Tada H, Paris PC, Erwin GR (2000) *The Stress Analysis of Cracks Handbook*, New York: ASME Press.

16. Muskhelishvili NI (1963) *Some Basic Problems of Mathematical Theory of Elasticity*, Leiden: P. Noordhoff.

17. Byrd PF, Friedman MD (1971) *Handbook of Elliptical Integrals for Engineers and Scientists*, New York Heidelberg Berlin: Springer-Verlag.

18. Feng XQ, Gross D (2000) On the coalescence of collinear cracks in quasi-brittle materials. *Eng Fract Mech* 65: 511–524.

AIMS Press